BJRS
BRAZILIAN JOURNAL OF RADIATION SCIENCES

doi.org/10.15392/2319-0612.2024.2643
2024, 12(4B) | 01-20 | e2643
Submitted: 2024-08-27
Accepted: 2025-04-07

Steady-State Coupled Calculations (Serpent-GeN-FOAM) Applied to Molten Salt Fast Reactor (MSFR)

Viera[a*], T. A. S.; Cruz[a], G. L.; Carvalho[a], Y, M.; Silva[a], G. C.; Carvalho[a], K. A.; Gonçalves[a], R. C.; Silva[a], V. V. A.; Barros[a], G.P.; Santos[a], A. A. C.

[a]Centro de Desenvolvimento da Tecnologia Nuclear

[*]Correpondence: tiago.vieira.eng@gmail.com

Abstract: The Molten Salt Fast Reactor (MSFR) represents a significant innovation within the Generation IV nuclear reactor systems, distinguished by its use of molten salt as both fuel and coolant. This study presents a methodology for performing steady-state coupled neutronics and thermal-hydraulics (TH) calculations for the Molten Salt Fast Reactor (MSFR) using Monte Carlo (MC) and Computational Fluid Dynamics (CFD) techniques. The reactor was fed with fuel salt using LiF as base salt, thorium (232Th) as a fertile material and 233U as fissile material. Uncertainty quantification was performed using an extended Grid Convergence Index (GCI) method. The extended Grid Convergence Index (GCI) method was applied to quantify uncertainties in temperature, velocity, and power density profiles. The results highlight the significance of coupled convergence, particularly for the power density field, and reveal lateral recirculation and hot spot formation in the reactor core. The noise reduction techniques applied to the MC simulations effectively smoothed power density profiles, reducing statistical uncertainty.

Keywords: Molten Salt Fast Reactor, Monte Carlo, CFD, Extended GCI, Thorium-based fuel.

SBPR

BJRS
BRAZILIAN JOURNAL OF RADIATION SCIENCES

doi.org/10.15392/2319-0612.2024.2643
2024, 12(4B) | 01-20 | e2643
Submitted: 2024-08-27
Accepted: 2025-04-07

Cálculos Acoplados em Regime Permanente (Serpent-GeN-FOAM) Aplicados ao Molten Salt Fast Reactor (MSFR)

Resumo: O Molten Salt Fast Reactor (MSFR) representa uma inovação significativa dentro dos sistemas de reatores nucleares de quarta geração, distinguindo-se pelo uso de sal fundido como combustível e refrigerante. Este estudo apresenta uma metodologia para realizar cálculos acoplados em estado estacionário de neutrônica e termo-hidráulica (TH) para o Molten Salt Fast Reactor (MSFR) utilizando técnicas de Monte Carlo (MC) e Fluido Dinâmica Computacional (CFD). O reator foi alimentado com sal combustível utilizando LiF como sal base, tório (^{232}Th) como material fértil e ^{233}U como material físsil. O cálculo de incertezas foi realizado utilizando Grid Convergence Index (GCI). O método GCI foi aplicado para quantificar incertezas nos perfis de temperatura, velocidade e densidade de potência. Os resultados destacam a importância da convergência acoplada, particularmente para o campo de densidade de potência, e revelam recirculação lateral e formação de pontos quentes no núcleo do reator. As técnicas de redução de ruído aplicadas às simulações MC suavizaram efetivamente os perfis de densidade de potência, reduzindo a incerteza estatística.

Palavras-chave: Molten Salt Fast Reactor, Monte Carlo, CFD, GCI extendido, Combustível a base de tório.

SBPR

1. INTRODUCTION

The Molten Salt Fast Reactor (MSFR) is a promising breakthrough technology selected by the Generation IV International Forum (GIF) as part of the Molten Salt Reactors (MSR) designs [1]. Unlike conventional nuclear reactors that use solid fuel rods, MSRs use a mixture of molten salt as both fuel and coolant, with fissile and fertile materials dissolved in the base salt, which circulates through the reactor core [2]. This design allows MSRs to operate at higher temperatures, thereby increasing electricity generation efficiency, and offering potential safety and economic benefits [3].

The MSFR specifically operates with a fast neutron spectrum and utilizes a fuel salt, primarily Lithium Fluoride (LiF), which can incorporate various fissile and fertile materials, including thorium (^{232}Th) and uranium-233 (^{233}U) [4]. It can also burn reprocessed fuel from traditional Pressurized Water Reactors (PWRs) [5]. The primary circuit of the MSFR circulates the fuel salt upward through the core cavity and downward through heat exchangers located circumferentially around the core. The flow of the fuel salt is perfomed by 16 pumps placed radially before the heat exchangers.

A unique feature of MSRs is the continuous circulation of liquid fuel, which significantly influences neutronics and thermal-hydraulics (TH) [6]. This intrinsic linkage necessitates a comprehensive understanding of reactor behavior, emphasizing the need for coupled calculations between these study areas. Accurate reactor TH analysis depends on precise power distribution derived from neutronics analysis, which is achieved through coupling TH and neutronics codes. This involves careful selection of codes, coupling schemes, and convergence criteria [7].

This work presents a methodology for performing steady-state coupled calculations between neutronics (Monte Carlo - MC) and TH (Computational Fluid Dynamics - CFD)

using a stable convergent scheme. Previous tests on a solid fuel reactor validate the methodology [8], and the achieved results of the current paper shows the hot spots within the cavity and the influence of coupled convergence on power density, velocity, and temperature profiles. The integration of CFD and MC methods is facilitated by mesh utilization by MC codes, enabling direct 1:1 grid coupling with CFD and eliminating the need for geometrical mapping [9]. Additionally, discretization uncertainty was estimated using the extended Grid Convergence Index (GCI) method to ensure the accuracy and reliability of the results.

2. METHODOLOGY

The present paper employs an external loose coupling scheme via file exchange according to [10, 11]. Serpent [12] handles neutronics (MC) while GeN-FOAM (TH) [13] manages thermal-hydraulics.

The methodology description is divided into three parts:

- Molten Salt Fast Reactor (MSFR) model;
- Coupled scheme and calculations parameters;
- The extended GCI method.

2.1. Molten Salt Fast Reactor (MSFR) model

The MSFR geometry and meshes were generated using the GMSH code [14]. GMSH is a free finite element mesh generator designed to build solid geometry representation initially from the Boundary Representation (B-REP) method. The dimensions of the MSFR cavity are shown in Figure 1. The developed MSFR model and mesh were based on files in the repository presented by Giudicelli [15].

Figure 1: Radial half slice of the MSFR cavity dimensions (cm).

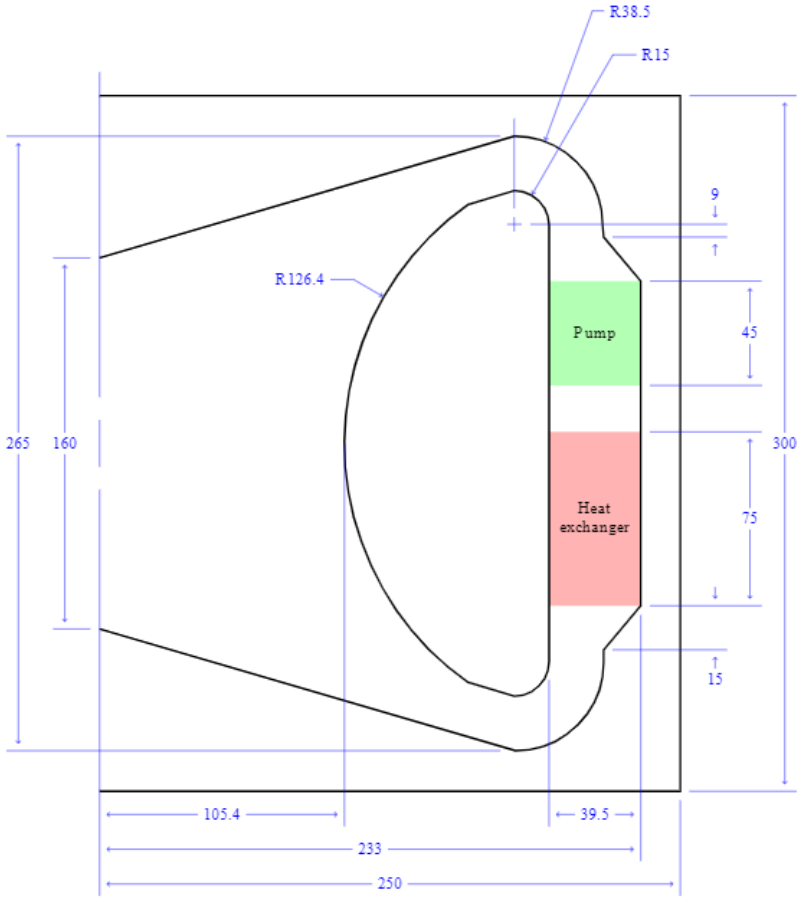

Source : (Giudicelli et al., 2022) [15].

Figure 2 depicts the development of a mesh-based model, taking into account the design characteristics and dimensions exhibited in Figure 1. In the simulations using the mesh presented in Figure 2, the CFD analysis was restricted to the fuel salt domain. This limitation aimed to save computational resources during calculations. The modeling approach adheres to a conservative methodology, where all heat generated within the core is presumed to be internally distributed rather than undergoing partial conduction to other existing materials.

Figure 2 elucidates the various domains incorporated into the model and shows the coarser generated mesh for MSFR (finer meshes cannot be seen due to cell density). Moreover, the developed model does not encompass heat exchangers or pumps, as these

parameters are not available in the existing literature [16, 17]. The simplifications adopted in the MSFR models in this study align with existing literature [18, 19, 20].

The MC simulations incorporated the entire geometric configuration, as the presence of reflectors and the fertile blanket exert a direct influence on the neutronic behavior of the reactor. Nevertheless, the temperature and density distributions were exclusively computed and incorporated within the fuel salt domain, leveraging the TH resolution. In contrast, the temperature and densities of the remaining materials were maintained at constant values throughout the simulations.

Figure 2: Geometry, boundary conditions and mesh of the MSFR.

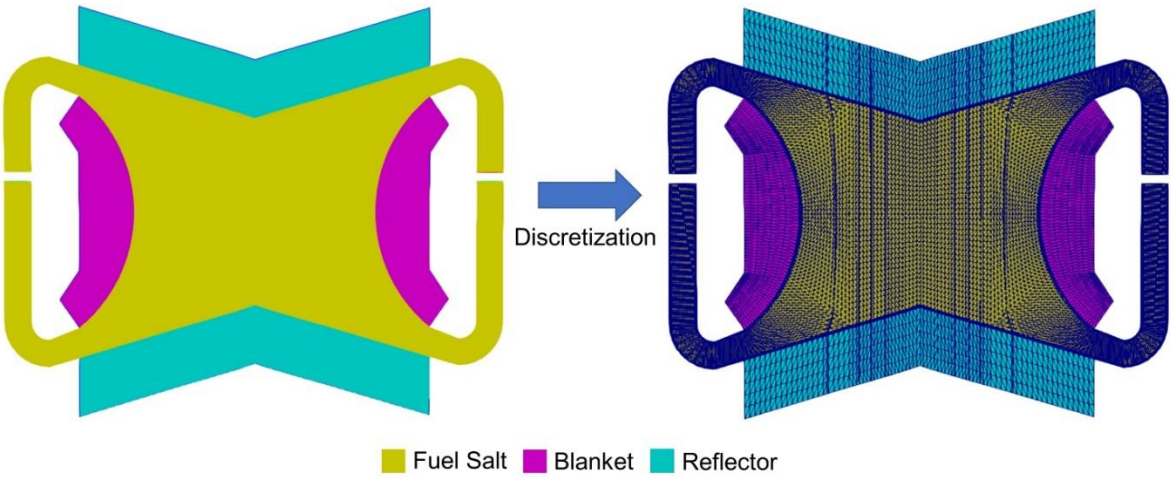

2.2. Coupled scheme and calculations parameters

The theoretical framework for this study begins with constructing CAD models of the MSFR reactor. This geometry is then discretized to generate meshes, which are used in an iterative coupling scheme to solve the thermal-hydraulics (TH) partial differential equations and neutron distribution (neutronics). The coupled solution, derived from successively refined meshes, is employed in the extended GCI step. This process results in highly detailed fields (temperature, velocity, and power density), which are converged with a fine mesh (1:1) and their respective numerical uncertainty.

The selected codes for this task were Serpent for neutronics [12] and GeN-FOAM for TH [13]. Serpent is a three-dimensional, continuous-energy Monte Carlo neutron transport code equipped with a multiphysics interface, which facilitates direct communication with CFD codes like OpenFOAM [9]. GeN-FOAM is a multi-physics solver for reactor analysis, based on OpenFOAM, and is capable of reading Serpent output volumetric power files [21].

The study employs an external loose coupling scheme via file exchange [10, 11]. Although it is not the most efficient method for coupled computations [7], it is suitable for this purpose because the time required for file exchanges is relatively short compared to TH and neutronics calculations.

This coupling approach, previously validated for steady-state convergence [22, 8] involves Serpent providing power distribution to the TH solver GeN-FOAM. GeN-FOAM then returns updated density and temperature fields until convergence is achieved. The scalar neutron flux is monitored to ensure convergence and to maintain a difference of less than 0.02% between successive iteration steps [10].

Although coupled convergence is stable with this algorithm, it does not guarantee minimal noise in MC results. Therefore, after achieving coupled convergence, further neutronic simulations are conducted until power density profiles present smoothness, with the number of neutrons incremented to 5E+05 to achieve this.

The neutronic parameters and materials composition were the same as used in [23]. For the neutronics simulations, the power value used in the MSFR was 2.7959 GW, taken from [4]. All simulations were performed with 100 active cycles and 10 inactive cycles, with the number of neutrons increasing from an initial 500 to 5E+05 for noise reduction. The nuclear data library used was ENDF/B-VII.1 [24], with materials temperatures set at 900 K. The compositions of the blanket salt, reflector, and fuel salt for the MSFR reactor are detailed in the Table 1, 2 and 3, respectively.

GeN-FOAM takes into account the thermal-physical properties of the fuel salt [2]. Boundary conditions for CFD simulations included an inlet temperature of 900 K, mass flow rates, and adiabatic non-slip walls. These TH parameters were derived from previous studies [4]. The TH convergence was reached within 800 iteration steps with an RMS residual of approximately 10E-07. The thermal-physical properties of the fuel salt and boundary conditions for CFD simulations are presented in Table 4 and 5, respectively.

Table 1: Blanket salt composition [2].

Composition	mol (%)
LiF	77.5
Th	22.5

Table 2: Reflector Ni alloy composition [2].

Element	atomic (%)
Ni	79,432
W	9,976
Cr	8,014
Mo	0,736
Fe	0,632
Ti	0,295
C	0,294
Mn	0,257
Si	0,252
Al	0,052
B	0,033
P	0,023
S	0,004

Table 3: Fuel salt initial composition for MSFR model.

Fuel Salt	mol (%)
LiF + Th + ^{233}U	LiF -77.5 Th – 19.7 ^{233}U – 2.8

Table 4: Fuel salt thermal-physical properties for MSFR model [2].

Property	Equation	Validity range (K)
Specific heat (J/KgK)	$Cp(T) = (-1.111 + 0.00278T)10^{-3}$	891 - 1020
Thermal conductivity (W/mK)	$\Lambda(T) = 0.928 + 8.397.10^{-5}T$	891 -1020
Density (kg/m)	$\rho(T) = 4.094 - 8.82.10^{-4}(T - 1008)$	893 - 1123
Dynamic viscosity (sPa)	$\nu(T) = 5.54.10^{-8} \exp(3689/T)$	898 - 1119

Table 5: Boundary conditions applied on CFD calculations for MSFR model [4].

Boundary	Condition
Inlet	Temperature = 900 (K) Mass flow rate = 18923.2 (kg/s)
Outlet	Pressure = 0 (Pa)
Walls	Adiabatic non-slip walls

2.3. The extended GCI method

The extended GCI method necessitates the use of a minimum of three successively refined meshes [25, 26, 27]. The parameters of the MSFR mesh-based models are detailed in Table 6, with h_i representing the mesh size and *r* the refinement ratio between meshes.

Table 6: Mesh-based parameters of MSFR model.

Mesh	h_i (m)	Number of cells	r_i
1	2.21E-02	2.8633E+06	1.26
2	2.78E-02	1.4377E+06	1.26
3	3.51E-02	7.1520E+05	-

In Equation (1), *N* represents the total count of cells employed for the computations, and V_i is the volume of the i^{th} cell. In Equation (2), the subscript 1, 2, 3, designates the transition from the finer to the coarser mesh.

$$h = \left[\left(\sum_{i=1}^{N} \Delta V_i\right) \Big/ N\right]^{1/3}, \tag{1}$$

$$r_{21} = \frac{h_2}{h_1}, \qquad r_{32} = \frac{h_3}{h_2}. \tag{2}$$

Initially intended for CFD applications, the GCI method, based on Richardson Extrapolation, can also be applied to Monte Carlo mesh-based calculations [25]. This method is employed to determine numerical uncertainty by following steps such as computing representative mesh sizes (*h*) and mesh refinement ratios (*r*) and calculating the discrepancy (Ɛ) between mesh results, as defined by Equation (3).

$$\varepsilon_{21} = |\gamma_2 - \gamma_1|, \quad \varepsilon_{32} = |\gamma_3 - \gamma_2| \,. \tag{3}$$

The apparent order of mesh convergence (*p*) is determined iteratively using Equations (4), (5), and (6).

$$p = \left[\frac{1}{\ln(r_{21})}\right]\left[ln\left|\frac{\varepsilon_{32}}{\varepsilon_{21}}\right| + q(p)\right], \tag{4}$$

$$q(p) = \ln\left[r_{32}^{p} - \frac{s}{r_{21}^{p}} - s\right], \tag{5}$$

$$s = 1.sign(\varepsilon_{21}/\varepsilon_{32}) \,. \tag{6}$$

The extended GCI value is then calculated using Equation (7), with a safety factor (*Fs*) of 1.25 for neutronics calculations.

$$GCI = \frac{Fs\varepsilon_{21}}{r_{21}^{p} - 1}. \tag{7}$$

The expanded uncertainty (U_d) for a 95% confidence interval due to grid generation is equal to the GCI value (Equation 8). Neutronics calculations produce their statistical confidence intervals, which can be combined with the GCI value for a total uncertainty assessment using Equation 9. In this study, GCI and neutronics confidence intervals are presented separately.

$$U_d = GCI\ , \tag{8}$$

$$U_{Total} = [(GCI_{Neutronics})^2 + (MC_{Neutronics})^2\ ]^{1/2}\ . \tag{9}$$

Upon completing the extended GCI procedure, a 95% confidence interval is established for the first meshes of the MSFR model, specifically for temperature, velocity, and power density slices.

3. RESULTS AND DISCUSSIONS

3.1. Neutronics Analysis

The convergence of the coupled calculations was performed by monitoring the scalar neutron flux variation through the iterations. However, by the end of this process, the power density profiles are still noisy, due to the intrinsic characteristic of MC calculations. Thus, the noise reduction process takes place to produce smooth results.

Figure 3 presents the entire process from coupled convergence to noise reduction. As noticeable, only power density profiles are shown since no sensible variation in temperature and velocity profiles through the iterations has been identified.

Figure 3: Noise reduction process impact on power density field for MSFR.

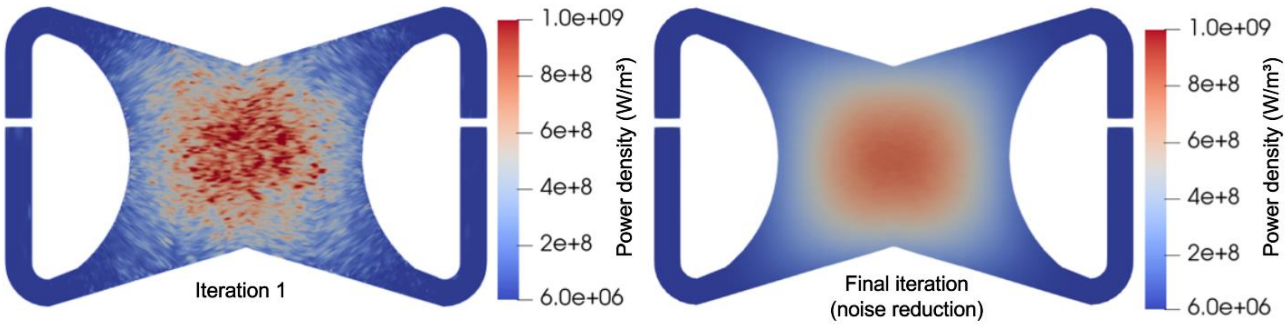

Regarding the power density field, it displays pronounced sensitivity to the iterative steps. This phenomenon arises from the incremental augmentation of sample size (number of neutron histories) in each iteration, resulting in a reduction of solution noise. This underscores the significance of the convergence step incorporated in the applied methodology.

Figure 4 shows the MSFR power density profile and its respective discretization uncertainty. In this figure, it is possible to verify that the power profile is converged and with low noise (see also Figure 3). The achieved power profile is in numerical accordance with the available literature [28, 29, 30], and the uncertainty remains small, particularly in the hot and cold legs of the reactor.

Figure 4: Power density slice for MSFR mesh 1 with discretization uncertainty.

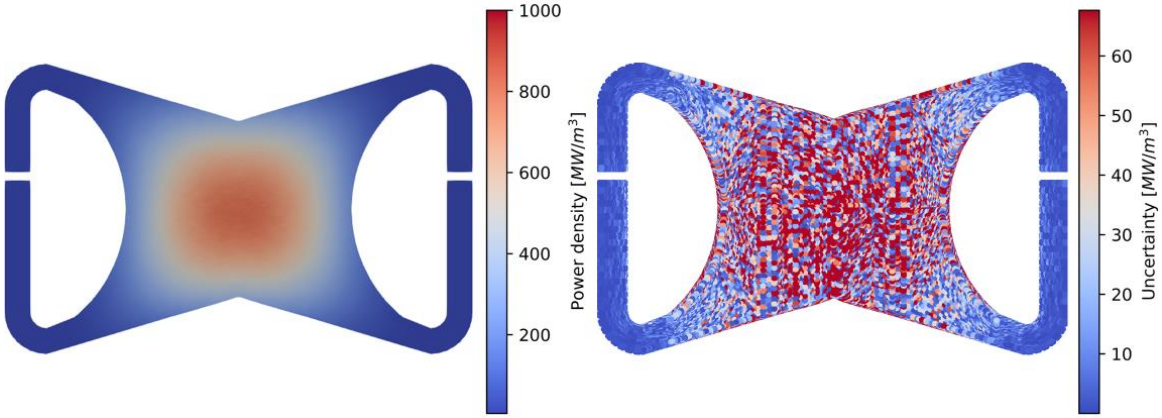

3.2. Thermal-hydraulics

Figure 5 illustrates the MSFR temperature profile along with its discretization uncertainty. The central part of the reactor exhibits higher temperatures, creating localized hot spots. These hot spots are particularly undesirable near the top and bottom reflector walls due to the engineering challenges they present, such as thermal stress and material degradation, which could compromise the structural integrity and long-term reliability of reactor components in these areas. It is important to note that, as referenced in [31], maintaining the reactor's operating temperature within the range of 750 to 800°C is crucial, as exceeding 800°C can lead to rapid salt corrosion, significantly intensifying beyond this threshold.

Figure 5: Temperature slice for MSFR mesh 1 with discretization uncertainty.

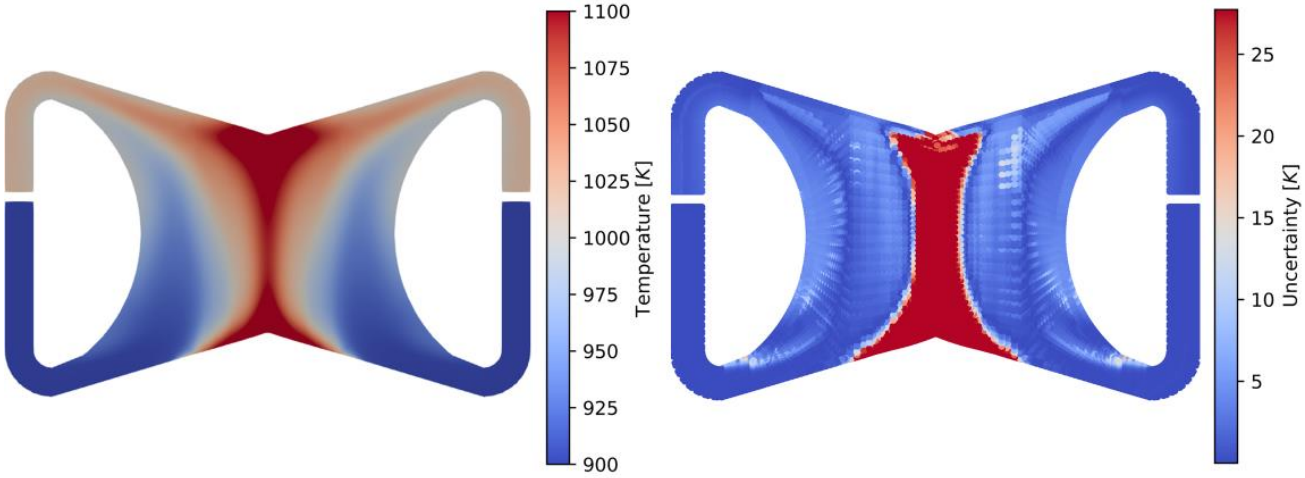

Even with the simplifications of the current model, the temperature profile shown in Figure 5 aligns with the findings of [4], [32] and [33]. However, a precise quantitative comparison cannot be made due to a lack of uniformity in the results of the reviewed literature. The reviewed literature has several differences, such as temperature ranges, coupled schemes, used codes, mapping schemes for boundaries, etc.

The temperature field depicted in Figure 5 corroborates the observation that recirculation points identified in the velocity field are the underlying cause of the observed hot spots. Notably, these hot spots exhibit heightened intensity in the central region of the reactor, particularly along the upper and lower walls.

Regarding discretization uncertainty, the profile in Figure 5 indicates higher values in the central part of the MSFR core, suggesting a lack of asymptotic convergence in the results from the meshes used. Nevertheless, the numerical uncertainty values are two orders of magnitude smaller than the peak temperature value.

The velocity profile and its uncertainty for the MSFR are presented in Figure 6. The velocity profile reveals lateral recirculation regions near the walls, with additional recirculation and stagnation regions observed in the bottom and top central parts of the core cavity, respectively. These low-velocity regions contribute to the hot spots seen in Figure 5.

The velocity uncertainty is distributed across several regions of the core, with higher velocities correlating to higher uncertainties.

Figure 6: Velocity slice for MSFR mesh 1 with discretization uncertainty.

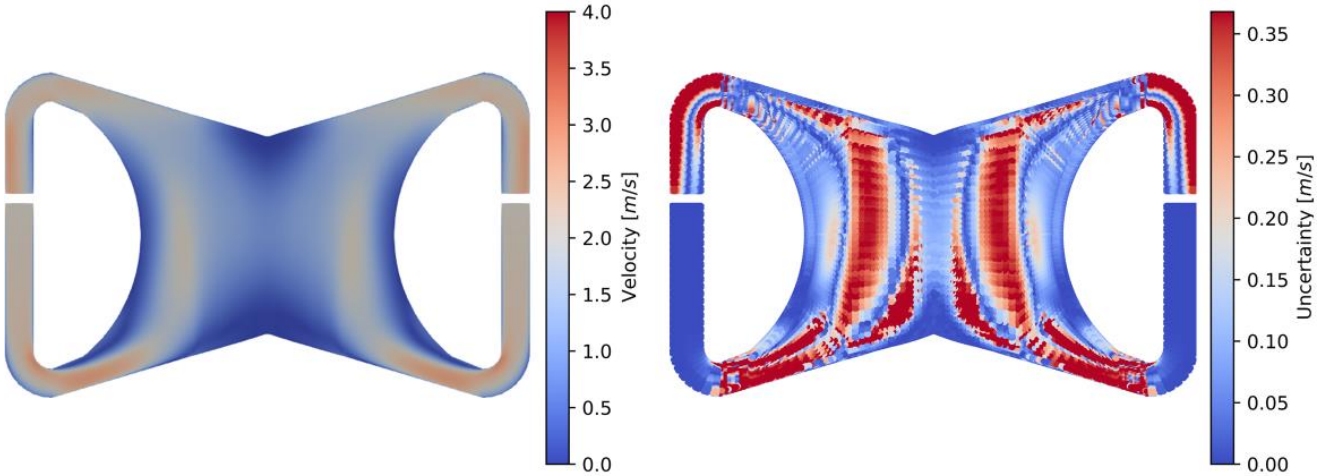

Figure 7 illustrates the recirculation and stagnation spots within the MSFR velocity field. Notable recirculation spots include one near the cold leg, close to the wall and another in the bottom central part of the core, along with a stagnation spot in the top central part of the core. The recirculation near the cold leg is characterized by a vortex between the wall and the high-velocity stream. The central bottom recirculation occurs due to the ascending velocity stream, causing the flow to detach from the bottom walls. The central top stagnation spot is a low-velocity region due to the direction of the velocity stream.

Figure 7: Velocity stagnation and recirculation spots for MSFR mesh 1.

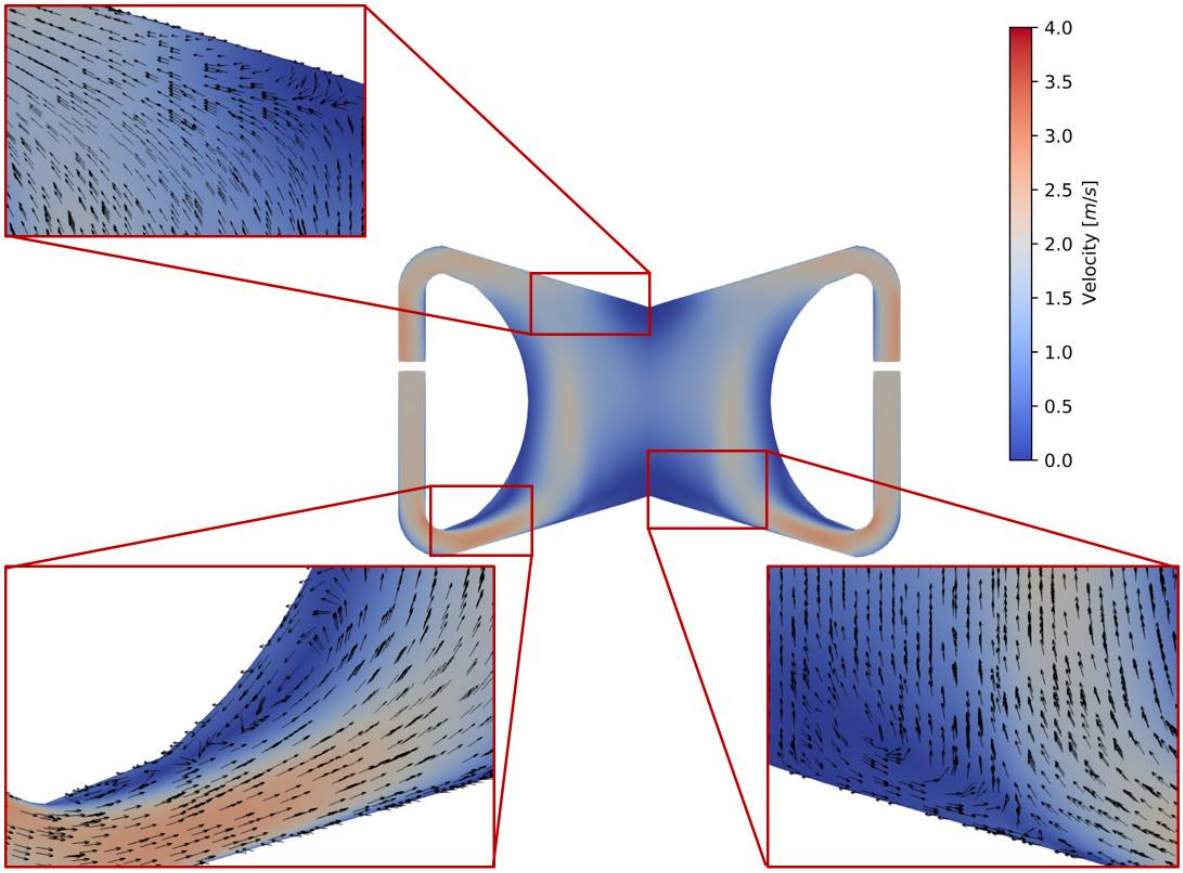

4. CONCLUSIONS

This work introduces a methodology for performing steady-state coupled calculations between MC and CFD, demonstrating its applicability to the MSFR. Utilizing a stable and convergent scheme, the methodology produced consistent and reliable outcomes, revealing hot spots within the MSFR cavity and underscoring the importance of coupled convergence in the power density, velocity, and temperature profiles. Discretization uncertainties were quantified using an extended GCI approach, ensuring the accuracy and reliability of both TH and neutronics parameters in the coupled calculations.

The results show that the velocity and temperature fields exhibit lower sensitivity to iterations compared to the power density field. The velocity profile identified lateral

recirculation regions near the walls, as well as recirculation and stagnation spots in the core's central parts. These recirculation phenomena contribute to the hot spots observed in the temperature field, particularly along the reactor's upper and lower walls. The power density field emphasized the importance of neutronic convergence, achieving a smooth and uniform profile by the final iteration.

The fine-mesh 1:1 CFD-MC calculations were convergent, demonstrating the efficacy of the noise reduction step in producing smooth power density profiles and reducing MC statistical uncertainty. In terms of computational cost, the MC noise reduction step was the major contributor, while the cost of file exchange steps decreased with larger mesh sizes. The computational expense of neutronics coupled calculations remained constant relative to the total time, with TH simulations becoming less significant as mesh refinement increases.

These findings provide a comprehensive understanding of the MSFR's performance under steady-state conditions, setting the stage for future research. Upcoming studies will explore the MSFR under various scenarios, such as pump failures and variations in mass flow and reactivity, and burnup analyses to evaluate the reactor's performance in terms of energy production and fissile material generation.

ACKNOWLEDGMENT

The authors are grateful to Brazilian research funding agencies CNEN – Comissão Nacional de Energia Nuclear, CNPq – Conselho Nacional de Desenvolvimento Científico e Tecnológico, CAPES – Coordenação de Aperfeiçoamento de Pessoal de Nível Superior, FAPEMIG – Fundação de Amparo à Pesquisa do Estado de Minas Gerais and FINEP - Financiadora de Estudos e Projetos for the support.

CONFLICT OF INTEREST

The authors declare that they have no competing financial interests or personal relationships that may have influenced the work reported in this study.

REFERENCES

[1] Kelly, J. E. Generation IV International Forum: A decade of progress through international cooperation. **Progress in Nuclear Energy**, Elsevier, v. 77, p. 240-246, 2014.

[2] Brovchenko, M. et al. Neutronic benchmark of the molten salt fast reactor in the frame of the EVOL and MARS collaborative projects. **EPJ N-Nuclear Sciences & Technologies**, Springer, v. 5, p. 2, 2019.

[3] Siemer, D. D. Why the molten salt fast reactor (MSFR) is the "best" Gen IV reactor. **Energy Science & Engineering**, Wiley Online Library, v. 3, n. 2, p. 83-97, 2015.

[4] Rouch, H., Geoffroy, O., Rubiolo, P., Laureau, A., Brovchenko, M., Heuer, D., & Merle-Lucotte, E. Preliminary thermal-hydraulic core design of the Molten Salt Fast Reactor (MSFR). **Annals of Nuclear Energy**, Elsevier, v. 64, p. 449-456, 2014.

[5] Fiorina, C., Aufiero, M., Cammi, A., Franceschini, F., Krepel, J., Luzzi, L., Mikityuk, K., & Ricotti, M. E. Investigation of the MSFR core physics and fuel cycle characteristics. **Progress in Nuclear Energy**, Elsevier, v. 68, p. 153-168, 2013.

[6] Aufiero, M. Development of advanced simulation tools for circulating fuel nuclear reactors. Politecnico di Milano, Milan & Italy, 2014.

[7] Vasconcelos, V., Santos, A., Campolina, D., Theler, G., & Pereira, C. Coupled unstructured fine-mesh neutronics and thermal-hydraulics methodology using open software: A proof-of-concept. **Annals of Nuclear Energy**, Elsevier, v. 115, p. 173-185, 2018.

[8] Vieira, T. et al. Study of a fine-mesh 1:1 Computational Fluid Dynamics-Monte Carlo neutron transport coupling method with discretization uncertainty estimation. **Annals of Nuclear Energy**, Elsevier, v. 148, p. 107-118, 2020.

[9] Leppänen, J., Valtavirta, V., Viitanen, T., & Aufiero, M. Unstructured Mesh Based Multi-Physics Interface for CFD Code Coupling in the Serpent 2 Monte Carlo Code. In Proceedings of the Conference, 2014.

[10] Gill, D. F. et al. Numerical Methods in Coupled Monte Carlo and ThermalHydraulic Calculations. Nuclear Science and Engineering, Taylor & Francis, v. 185, p. 194-205, 2017.

[11] Wang, J. et al. Review on neutronic/thermal-hydraulic coupling simulation methods for nuclear reactor analysis. **Annals of Nuclear Energy**, Elsevier, v. 137, p. 107-165, 2020.

[12] Leppänen, J. Development of a new Monte Carlo reactor Physics Code. Helsinki University of Technology, Espoo & Finland, 2007.

[13] Fiorina, C. et al. GeN-Foam: a novel OpenFOAM-based multi-physics solver for 2D/3D transient analysis of nuclear reactors. **Nuclear Engineering and Design**, Elsevier, v. 294, p. 24-37, 2015.

[14] Geuzaine, C., & Remacle, J.-F. Gmsh: A 3-D Finite Element Mesh Generator with Built-in Pre- and Post-Processing Facilities**. International Journal for Numerical Methods in Engineering**, Wiley, v. 79, p. 1309-1331, 2009.

[15] Giudicelli, G., Permann, C., Gaston, D., Abou-Jaoude, A., & Feng, B. The Virtual Test Bed (VTB) repository: a library of multiphysics reference reactor models using NEAMS tools. In Proceedings of the International Conference on Physics of Reactors - PHYSOR 2022, 2022.

[16] Di Ronco, A., Giacobbo, F., Lomonaco, G., Lorenzi, S., Wang, X., & Cammi, A. Preliminary analysis and design of the energy conversion system for the Molten Salt Fast Reactor. Sustainability, Multidisciplinary Digital Publishing Institute, v. 12, n. 24, p. 10497, 2020.

[17] Aufiero, M., Cammi, A., Geoffroy, O., Losa, M., Luzzi, L., Ricotti, M. E., & Rouch, H. Development of an OpenFOAM model for the Molten Salt Fast Reactor transient analysis. **Chemical Engineering Science, Elsevier**, v. 111, p. 390-401, 2014.

[18] Laureau, A., Heuer, D., Merle-Lucotte, E., Rubiolo, P. R., Allibert, M., & Aufiero, M. Transient coupled calculations of the Molten Salt Fast Reactor using the transient fission matrix approach. **Nuclear Engineering and Design**, Elsevier, v. 316, p. 112-124, 2017.

[19] Tiberga, M. Development of a high-fidelity multi-physics simulation tool for liquid-fuel fast nuclear reactors. Ph.D. thesis, TU Delft University, **Energy and Nuclear Engineering**, 2020.

[20] Gonzalez Gonzaga De Oliveira, R. Improved methodology for analysis and design of Molten Salt Reactors. Ph.D. thesis, EPFL, 2021.

[21] OpenFOAM - the Open Source CFD Toolbox: User Guide, Version 2212, Jul. 2022.

[22] Dufëk, J., & Hoogenboom, J. Description of a stable scheme for steady-state coupled Monte Carlo-thermal-hydraulic calculations. **Annals of Nuclear Energy**, Elsevier, v. 68, p. 1-3, 2014.

[23] Vieira, T. A. S., Ribeiro, F. R. C., Carvalho, Y. M., Silva, V. V. A., de Paula Barros, G., & dos Santos, A. A. C. Investigation of discretization uncertainty in Monte Carlo neutron transport simulations of the Molten Salt Fast Reactor (MSFR). **Brazilian Journal of Radiation Sciences**, v. 11, n. 4, p. 01-27, 2023.

[24] Chadwick, M. B. et al. ENDF/B-VII.1 Nuclear Data for Science and Technology: Cross Sections, Covariances, Fission Product Yields and Decay Data. **Nuclear Data Sheets**, Elsevier, v. 112, n. 12, p. 2887-2996, 2011.

[25] Roache, P. J. Fundamentals of Verification and Validation. Hermosa Publishers, Socorro, NM, 2009.

[26] Celik, I., Ghia, U., Roache, P. J., Freitas, C., Coloman, H., & Raad, P. Procedure of Estimation and Reporting of Uncertainty Due to Discretization in CFD Applications. **Journal of Fluids Engineering**, ASME, v. 130, p. 078001, 2008.

[27] Matozinhos, C., & Campagnole dos Santos, A. Two-phase CFD simulation of research reactor siphon breakers: A verification, validation and applicability study. **Nuclear Engineering and Design**, Elsevier, v. 326, 2018.

[28] Aufiero, M. Development of advanced simulation tools for circulating fuel nuclear reactors. Ph.D. thesis, Politecnico di Milano, 2014.

[29] Allibert, M., Aufiero, M., Brovchenko, M., Delpech, S., Ghetta, V., Heuer, D., Laureau, A., & Merle-Lucotte, E. Molten salt fast reactors. **In Handbook of Generation IV Nuclear Reactors**, Elsevier, p. 157-188, 2016.

[30] Alsayyari, F., Tiberga, M., Perkó, Z., Kloosterman, J. L., & Lathouwers, D. Analysis of the Molten Salt Fast Reactor using reduced-order models. **Progress in Nuclear Energy**, Elsevier, v. 140, p. 103909, 2021.

[31] Wright, R. N., & Sham, T.-L. Status of metallic structural materials for molten salt reactors. Idaho National Lab (INL), Idaho Falls, ID (United States); Argonne National Lab, 2018.

[32] Abou-Jaoude, A., Harper, S., Giudicelli, G., Balestra, P., Schunert, S., Martin, N., Lindsay, A., Tano, M., & Freile, R. A workflow leveraging MOOSE transient multiphysics simulations to evaluate the impact of thermophysical property uncertainties on molten-salt reactors. **Annals of Nuclear Energy, Elsevier**, v. 163, p. 108546, 2021.

[33] German, P., Tano, M., Fiorina, C., & Ragusa, J. C. GeN-ROM—An OpenFOAM-based multiphysics reduced-order modeling framework for the analysis of Molten Salt Reactors. **Progress in Nuclear Energy**, Elsevier, v. 146, p. 104148, 2022.

LICENSE